RESULTS AND DISCUSSION

CHAPTER 4

RESULTS AND DISCUSSION

4.1 INTRODUCTION

Thin film characterization provides new challenges as they generally consist of a small amount of material, and thus pose problems from an analytical point of view. The measurement of thin film properties is indispensable for the study of thin film materials and devices. To make sure that coatings which were produced by a given process satisfy the specified technological demands a wide field of characterization, measurement and testing methods are available. The chemical composition, crystalline structure, optical properties, electrical properties and mechanical properties must be considered in thin film analysis. With the increasing interdisciplinary nature of application, demand for effective film characterization and property measurement in both individual films and multilayer coatings has recently been developed. There are a number of major considerations that determine the choice of an instrumental method to solve a specific problem in the surface analysis of thin films. The results obtained from UV-VIS spectrometry, Photoluminescence, XRD, GC- MS and SEM of the solution grown polymer thin film are discussed in this chapter.

4.2 ULTRAVIOLET AND VISIBLE SPECTROSCOPY

UV-Visible Spectroscopy is defined as the absorption and emission of radiation associated with changes in spatial distribution of electrons in an atom and molecules. In practice, the electrons involved are usually the valance or bonding electrons, which can be excited by absorption of UV or visible or near IR radiations. Excitation of bound electrons from the highest occupied molecular orbits increases the spatial extend of electron distribution, making the total electron density larger and often more polarizable. Ultra violet absorption spectra arise due to electronic excitation. The outer electron atoms or molecules absorb radiant energy and get excited. These electronic transitions are quantized and depend upon the electronic structure of absorber **(Patanian 2004).**

The ultraviolet region corresponds to 200-400nm and visible region to 400 - 800nm. On passing electromagnetic radiation in the ultraviolet and visible regions through a compound with multiple bonds, a portion of the radiation is normally absorbed by the compound. The amount of absorption depends on the wavelength of the radiation and the structure of the compound. The absorption of radiation is due to the subtraction of energy from the radiation beam when electrons in orbital of lower energy are excited into orbital of higher energy. Since this is an electron excitation phenomenon, UV-visible spectroscopy is called electronic spectroscopy **(P.S.Kalsi, 2009).**

EXPERIMENT

The experimental arrangement of a typical double beam UV-Visible spectrometer is shown in figure 4.1. A beam of light from a visible or UV light source (colored red) is separated into its component wavelengths by a prism or diffraction grating. Each monochromatic beam in turn is split into two equal intensity beams by a half-mirrored device. One beam is called as the sample beam and it passes through a small transparent container called the cuvette containing a solution of the compound being studied in a transparent solvent. The other beam called as the reference passes through an identical cuvette containing only the solvent. The intensities of these light beams are then measured by electronic detectors and then compared. The intensity of the reference beam which should have little or no light absorption is denoted as I_0. The intensity of the sample beam is I. The ultraviolet (UV) region scanned is normally from 200 to 400 nm and the visible portion is from 400 to 800 nm. Absorption may be presented as transmittance ($T = I/I_0$) or absorbance ($A = \log I_0/I$). If no absorption has occurred then T = 1.0 and A= 0. Different compounds may have different absorption maxima **(Skoog et.al, 2007).**

4.3 PHOTOLUMINESCENCE SPECTOSCOPY

Photoluminescence is a process in which a substance absorbs photons (electromagnetic radiation) and then re-radiates photons. Quantum mechanically, this can be described as an excitation to a higher energy state and then a return to a lower energy state accompanied by the emission of a photon. This is one of many forms of

luminescence (light emission) and is distinguished by photoexcitation (excitation by photons). The period between absorption and emission is typically extremely short, in the order of 10 nanoseconds. It is a two step process (i) excitation of electrons from a lower energy state to higher state as a result of absorption of energy, and (ii) emission of light radiation when the electrons fall back to a lower energy state. Photoluminescence systems are excited by the absorption of photons and they re-emit energy in the form of radiation of the wavelength which is same or longer than the wavelength used for excitation. If the wavelength radiation absorbed and emitted is exactly the same the phenomenon is termed as the resonance radiation or resonance luminescence. The PL spectroscopy is suitable for the characterization of both organic and inorganic materials of virtually any size and the samples can be in solid, liquid or gaseous forms (**Supriya S. Mahajan, 2010**). The basic principle of photoluminescence process is illustrated in figure 4.2.

Electromagnetic radiation in the UV and visible ranges is utilized in PL spectroscopy. The sample's PL emission properties were characterized by four parameters; intensity, emission wavelength, bandwidth of emission peak and the emission stability. The PL properties of a material can change in different ambient environments or in the presence of other molecules. Additionally, as the released photon corresponds to the energy difference between the states, PL spectroscopy can be utilized to study material properties such as band gap, recombination mechanisms and impurity levels. The schematic PL spectroscopy setup is shown in figure.4.3.

Sample is placed in a quartz cuvette with a known path length. Double beam optics is generally employed. The first beam passes through an excitation filter or monochromator, then through the sample and onto a detector. This impinging light causes photoluminescence, which is emitted in all directions. A small portion of the emitted light arrives at the detector after passing through an optional emission filter or monochromator. A second reference beam is attenuated and compared with the beam from the sample, then the PL spectrum is recorded in the signal processing unit. Solid samples can also be analysed, with the incident beam impinging on the material. Generally an emission spectrum is recorded, where the sample is irradiated with a single

wavelength and the intensity of the luminescence emission is recorded as a function of wavelength. In converse, the emission peaks are identified and fixed to scan over an excitation spectrum of wavelength to identify whether the emission is associated with one or more excitation.

4.4 X-RAY DIFFRACTION

There are vast array of physical methods for investigating the structure of solids, each technique with its own strengths and weaknesses. Among them XRD technique is most preferred to solve more crystalline structure than all the other techniques put together **(Y. Anjaneyulu at al., 2006).** X-ray powder diffraction is a non-destructive technique applied for the characterization of the crystalline materials. The method has been used for phase identification, quantitative analysis and the determination of structure imperfections. X-ray is based on the diffraction of radiation when they encounter small obstacles.

X-ray diffraction is based on constructive interference of monochromatic X-rays and a crystalline sample. These X-rays are generated by a cathode ray tube, filtered to produce monochromatic radiation, collimated to concentrate, and directed towards the sample. The interaction of the incident rays with the sample produces constructive interference when conditions satisfy Bragg's law which is given by

$$n\lambda = 2d \sin\theta$$

Where,

n is order of diffraction,

λ is the wavelength of X-rays,

d is the interplanar spacing generating the diffraction and

θ is the diffraction angle.

By varying the angle theta, the Bragg's Law conditions are satisfied by different d- spacings in polycrystalline materials. Based on the principle of X-ray diffraction, a

wealth of structural, physical and chemical information about the material investigated can be obtained. The X-Ray diffraction of Bragg law is shown on figure.4.4.

Generally speaking thin film diffraction refers not to a specific technique but rather a collection of XRD techniques used to characterize thin film samples grown on substrates. Thin film diffraction methods are used as important process development and control tools, as hard x-rays can penetrate through the epitaxial layers and measure the properties of both the film and the substrate.

WORKING OF X-RAY DIFRACTOMETER

The typical diffractometer system is illustrated in figure 4.5. The X-ray diffractometer consist of three basic elements such as an X-ray tube, a sample holder and an X-ray detector. X-rays are generated in a cathode ray tube by heating a filament to produce electrons, accelerating the electrons toward the target by applying a voltage and bombarding the target material with electrons. When electrons have sufficient energy to dislodge inner shell electrons of the target material, characteristic X-ray spectra are produced. These spectra consist of several components, the most common being $K\alpha$ and $K\beta$. $K\alpha_1$ has a slightly shorter wavelength and twice the intensity as $K\alpha_2$. Filtering by foils or crystal monochromator is required to produce monochromatic X-rays. The X-ray tube specimen and receiving slit also lie on the arc of the focusing circle. Unlike the goniometer circle which remains fixed the radius of the focusing circle is a function of θ-2θ with the radius decreasing as θ increases. The incident angle θ defined as the angle between the incident beam and the sample, and 2θ is the angle between the incident and diffracted beams. The detector is moved (rotated) at twice the angular rate of the sample to maintain the θ-2θ geometry. The filter is used to remove all but the desired $K\alpha$ radiation from the diffracted beam before it enters the detector. The geometry of an X-ray diffractometer is such that the sample rotates in the path of the collimated X-ray beam at an angle θ while the X-ray detector is mounted on an arm to collect the diffracted X-rays and rotates at an angle of 2θ.

4.5 GAS CHROMATOGRAPHY- MASS SPECTROMETRY

Gas Chromatography–Mass Spectrometry (GC-MS) is a method that combines the features of gas chromatography and mass spectrometry to identify different substances within a test sample. GC-MS has been widely accepted as a "gold standard" for chemical identification of volatile and semi-volatile organic compounds in mixtures, drug detection, environmental analysis, explosives investigation, and identification of unknown samples. Additionally, it can identify trace elements in materials that were previously thought go undetected by other technologies. GC can separate volatile and semi volatile compounds with great resolution, but it cannot identify them. MS can provide detailed structural information on most compounds such that they can be exactly identified, but it cannot readily separate them. Gas chromatography and mass spectrometry are, in many ways, highly compatible techniques. Because of its high sensitivity and fast scan speed, this technique is most suited to provide definite structural information from the small quantities of material eluted from a gas chromatograph. In both techniques, the sample is in the vapor phase, and both techniques deal with about the same amount of sample (typically less than 1 ng). Unfortunately, there is a major incompatibility between the two techniques: The compound exiting the gas chromatograph is a trace component in the GC's carrier gas at a pressure of about 760 torr, but the mass spectrometer operates at a vacuum of about 10^{-6} to 10^{-5} torr. This is a difference in pressure of 8 to 9 orders of magnitude, a considerable problem **(Frank A. Settle, 1997).**

INSTRUMENTATION

The typical GC-MS spectrometer is shown in figure.4.6. The GC-MS is composed of two major building blocks: the gas chromatograph and the mass spectrometer. The gas chromatograph utilizes a capillary column which depends on the column's dimensions (length, diameter, film thickness) as well as the phase properties. The difference in the chemical properties between different molecules in a mixture will separate the molecules as the sample travels the length of the column. The molecules are retained by the column and then elute from the column at different times (called the retention time), and this

allows the mass spectrometer downstream to capture, ionize, accelerate, deflect, and detect the ionized molecules separately. The mass spectrometer does this by breaking each molecule into ionized fragments and detecting these fragments using their mass to charge ratio.

These two components, used together, allow a much finer degree of substance identification than either unit used separately. It is not possible to make an accurate identification of a particular molecule by gas chromatography or mass spectrometry alone. The mass spectrometry process normally requires a very pure sample while gas chromatography using a traditional detector cannot differentiate between multiple molecules that happen to take the same amount of time to travel through the column (*i.e.* have the same retention time), which results in two or more molecules that co-elute. Sometimes two different molecules can also have a similar pattern of ionized fragments in a mass spectrometer (mass spectrum). Combining the two processes reduces the possibility of error, as it is extremely unlikely that two different molecules will behave in the same way in both a gas chromatograph and a mass spectrometer. Therefore, when an identifying mass spectrum appears at a characteristic retention time in a GC-MS analysis, it typically tends to increased certainty that the analyte of interest is in the sample.

4.6 SCANNING ELECTRON MICROSCOPY

Scanning electron microscopes are becoming more and more useful and popular for the direct observation of surfaces because they offer better resolution and depth of field than optical microscopes. A scanning electron microscope (SEM) is a type of electron microscope that images a sample by scanning it with a high-energy beam of electrons in a raster scan pattern. The electrons interact with the atoms that make up the sample producing signals that contain information about the sample's surface topography, composition, and other properties (**Maissel and Glang, 1983**). Accelerated electrons in an SEM carry significant amounts of kinetic energy, and this energy is dissipated as a variety of signals produced by electron-sample interactions when the incident electrons are decelerated in the solid sample. The types of signals produced by an SEM include secondary electrons, back-scattered electrons (BSE), characteristic X-rays, light

(cathodoluminescence), specimen current and transmitted electrons. Secondary electron detectors are common in all SEMs, but it is rare that a single machine would have detectors for all possible signals. The signals result from interactions of the electron beam with atoms at or near the surface of the sample. The output can be used to modulate the brightness of a cathode ray tube (CRT). Every point that the beam strikes on the sample is mapped directly onto a corresponding point on the screen. The principle image produced in the SEM is of three types, Secondary electron images, Backscattered electron images and Elemental X-ray maps.

Secondary and backscattered electrons are separated according to their energies. They are produced by different mechanisms. When a high energy primary electron interacts with an atom, it undergoes either inelastic scattering with atomic electrons or elastic scattering with atomic nucleus. In an elastic collision with an electron, some amount of energy is transferred to the other electron. If the energy transfer is very small, the emitted electron will probably not have enough energy to exit the surface. If the energy transferred exceeds the work function of the material, the emitted electron can exit the solid. When the energy of the emitted electron is less than about 50eV, by convention it is referred to as a Secondary Electron (SE), or simply a secondary. Most of the emitted secondaries are produced within the first few nm of the surface. Backscattered Electrons (BSEs) are considered to be the electrons that exit the specimen with an energy greater than 50eV, including Augur electrons. However most BSEs have energies comparable to the energy of the primary beam.

INSTRUMENTATION

The schematic representation of a Scanning Electron Microscope is shown in figure.4.7. Essential components of all SEMs include the following: Electron Source ("Gun"), Electron lenses, Sample stage, detectors for all signals of interest, display / data output devices. In a typical SEM, an electron beam is thermionically emitted from an electron gun fitted with a tungsten filament cathode. Tungsten is normally used in thermionic electron guns because it has the highest melting point and lowest vapour pressure of all metals, thereby allowing it to be heated for electron emission, and because

of its low cost. The electron beam, which typically has an energy ranging from 0.2 keV to 40 keV, is focused by one or two condenser lenses to a spot about 0.4 nm to 5 nm in diameter. The stream is condensed by the first condenser lens (usually controlled by the "coarse probe current knob"). This lens is used to both form the beam and limit the amount of current in the beam. The second condenser lens forms the electrons into a thin, tight, coherent beam and is usually controlled by the "fine probe current knob. The beam passes through pairs of scanning coils or pairs of deflector plates in the electron column.

The scan coils are energized (by varying the voltage produced by the scan generator) and create a magnetic field which deflects the beam back and forth in a controlled pattern. The varying voltage is also applied to the coils around the neck of the Cathode-ray tube (CRT) which produces a pattern of light deflected back and forth on the surface of the CRT. The pattern of deflection of the electron beam is the same as the pattern of deflection of the spot of light on the CRT. The final objective lens, which deflect the beam in the x and y axes so that it scans in a raster fashion over a rectangular area of the sample surface. The raster scanning of the CRT display is synchronised with that of the beam on the specimen in the microscope, and the resulting image is therefore a distribution map of the intensity of the signal being emitted from the scanned area of the specimen. The image may be captured by photography from a high-resolution cathode ray tube, but in modern machines the image is digitally captured and displayed on a computer monitor.

4.7 RESULTS OBTAINED

1. Observation from Film Thickness:

Microbalance Gravimetric is one of the simplest method for thickness measurement which was employed in this study. Thickness measurement was carried out for several samples deposited both by CBD and Spin coating. By measuring the mass of the substrate before and after deposition, the weight of the deposited film was calculated, and film thickness was calculated using the knowledge of deposited area and density of the material.

Thickness of the polymer films coated by CBD method are given in table 1, and it is observed that, film thickness increases as deposition time duration increases validating the technique adopted in this study. Similarly thickness of the spin coated films is shown in table 2, and is found to increase as time duration increases, but decreases as rpm increases.

2. UV-Visible spectrum results:

Ultraviolet (UV) and visible (VIS) light can cause electronic transitions. When a molecule absorbs UV-Vis radiation, the absorbed energy excites electron into an empty higher energy orbital. The absorbance of energy can be plotted against the wavelength to yield a UV-VIS spectrum. Most organic compounds that absorb UV-VIS radiation contain conjugated π-bonds. Both the shape of the peak (s) and the wavelength of maximum absorbance (λ_{max}) give information about the structure of the compound.

All UV-VIS spectrophotometric measurements of solution grown polymer films were made with LAMBDA UV/VIS spectrophotometer of Perkin-Elmer. The entire coated surface was illuminated by UV-VIS radiation, and the spectroscopic data was taken for sample I, II and III. UV-VIS spectroscopy is useful as an analytic technique for two reasons. First, it can be used to identify some functional groups in molecules. Secondly, it can be used for assaying i.e. determining the content and strength of a substance. The transmittance is defined as the ratio of the intensity of light that passes through the sample to the light intensity incident upon sample.

The UV-Visible-NIR spectra of PS films (sample I) is shown figure.4.8. The % transmittance was recorded upto the range of 2500nm. The transmittance spectrum reveals a peak at 298nm in the UV region and transmittance edge appears at 508 nm. The transmittance value increases as wavelength increases. The Transmittance spectrum of PMMA films (sample II) is shown in figure 4.9, maximum transmittance peak is found to occur at 294 nm and the transmittance curve increases as wavelength increases and it decreases around 2200 nm wavelength region. The transmittance spectrum of composite film (sample III) is shown in figure 4.10. A sharp intense peak is observed at 300 nm i.e. in UV region and transmittance increases gradually as wavelength increases.

3. PL spectrum results:

The study of optical absorption is a useful method for investigating the optical transitions and providing information about the band structure and optical energy gap of the materials. The principle of this technique is that the photons with energies higher than the band gap energy will be absorbed by the molecules and excited to the higher molecular orbitals and emission reflect the probability of transition. PL behaviour of all thin film samples deposited in this study are excited at 300 nm and emission spectrum is recorded from 318 nm to 587 nm. The photoluminescence behaviour of polystyrene film (sample I) is shown in figure.4.11 which shows a sharp emission at 539 nm. The PL spectrum of PMMA film is shown in figure.4.12, revealing prominent emission at 542 nm. The PL spectrum of composite (sample III) is shown in figure.4.13, which shows the emission occurence at 373 nm, 389 nm and 501 nm.

Discussion of UV-Visible and PL results:

The transmittance of PMMA is normally above 90%, the PMMA-PS composite in EMK exhibits transmittance around 90% and also has consistent transmittance over the entire IR range (~ 1000nm – 2400nm). Hence this feature of the film will be very much favorable for IR therapy. Comparing sample I and sample III, it is understood that the emission of PS at 539nm has shifted to 501nm in the composite (sample III). Pristine PS is noted to have an emission at 510 nm from the literature cited by Deepak et al. This indicates that addition of PMMA with PS in the present study has reduced the band gap from 510 nm to 501nm. The value of FWHM is 70 nm for composite, whereas the FWHM value of PMMA is 50 nm from UV-Vis spectra which is shown in figure.4.14.

An energy level diagram is shown in figure.4.15, considering the absorption and emission studies. It is seen from the reference of Deepak et al., that PMMA on excitation at 366 nm emits 458 nm, emission at 510 nm is observed when PS is excited at 337 nm. Excitation at 300 nm for the composite film deposited in this study shows emission at 373 nm, 389 nm and 501 nm, indicating a shift in emission peak.

The analysis of emission from sample I (PS), sample II (PMMA) and the sample III, composite of PMMA and PS in EMK shows the emission at 373 nm, 389 nm and 501

nm for the similar excitation at 300 nm. This suggests that PMMA/PS composite with especially the solvent used EMK can be a perspective candidate for UV pass filters. While looking at the FWHM of the absorption peaks, it is understood that the bandwidth has shifted from 50 nm to 70 nm, an additional 20 nm band broadening indicates that ample amount of transition probability has been allowed due to the composite film formation compared to PMMA films alone. Hence PS/PMMA composite films can act as UV pass filters in the solar simulator experiments and microbial activity studies.

4. Results of XRD analysis:

Diffraction and scattering from polymers present a set of problems different from those encountered with crystalline materials or even amorphous materials such as inorganic glasses. X-ray crystallographic techniques when applied to polymeric solids we obtain some interesting features of their internal structure also. It was found that good majority of polymers diffract X-rays like any crystalline substance but many behave like amorphous materials giving very broad and diffuse X-ray patterns. Unlike simple inorganic compounds, polymers do not have perfectly ordered crystal lattice formation and are not completely crystalline. Hence, the X-ray diffraction from them are found to be a mixture of sharp as well as diffused patterns **(Arora et al., 2003).**

The X-ray diffraction studies were carried out using Pananalytical Xpert pro X-ray diffractometer with CuKα radiation of wavelength λ=1.54060 Å in the angle range 2θ=10° to 80° with step size of 0.0170°. The X- ray diffraction pattern of sample I, II and III are shown in Figures.4.16, 4.17 and 4.18 respectively. XRD pattern of PMMA and composite shows only two broad peaks indicating amorphous nature. Table.3 shows the measured values of XRD parameters and the calculated values of interchain distance (r). Values of r have been calculated using the formula

$$r = \frac{5}{8}\frac{\lambda}{\sin\theta}$$

The interchain distance between PMMA polymer chain is 3.5295 Å (computed from first peak) and the distance between pendant groups ($COOCH_3$) is 1.5536 Å (computed from second peak) respectively.

5. Interpretation of GC-MS spectrum:

GC-MS is used both for the qualitative identification and for the quantitative measurement of individual components in complex mixtures. A mass spectrum is a presentation of the masses of positively charged fragments versus their relative concentrations. Mass spectrum is produced as a result of a series of competing and consecutive unimolar reactions. A graphic presentation or a plot of the spectrum may be used which represents the intensities of the signals at various m/e values. A single mass spectrum is equivalent to dozens of physical properties of that compound for identifying the structure. No two compounds can have exactly similar mass spectra.

The GC-MS spectrum of poly(methyl methacrylate) sample were obtained from the JEOL GCMATE II mass spectrometer using Chemical Ionization (CI) and Electron Impact (EI) source. The mass spectrum and the corresponding fragmentation spectrum are shown in figures from 4.19 to 4.25. Six peaks at 9.62, 14.23, 14.75, 16, 16.17 and 21.99 were observed in GC-MS. The mass spectrum of GC peak at 9.62 exhibits one (M-15) peak and one (M-28) peak which proves the presence of CH_3 and C=O groups. Also in the same (M-15), (M-28) peaks were observed on the mass spectrum of GC peaks at 16 and 16.17. Hence it can be concluded that the fractions at 9.62, 16 and 16.17 may be a methyl and carbonyl type of compound. The mass spectrum of the fraction at 14.75 exhibits one (M-28) and two (M-17) peaks, which indicates the presence of C=O and OH groups. Similarly (M-17) and (M-28) peaks correspond to C=O and OH groups were observed in the mass fraction at 21.99. Thus from the GC-MS spectrum the presence of functional groups of PMMA are identified.

6. SEM Analysis:

The surface morphology of composite PS/PMMA thin film was analysed using FEI Quanta FEG 200 High Resolution Scanning Electron Microscope (HRSEM), which

is shown in figure.4.26. The micrograph of the film indicates homogeneous, continuous and crack free nature of the surface. The film is found to have randomly oriented rod like grains. Both short and long rods are present in the SEM image of PS/PMMA composite film, having a length of 1.61μm and 2.89μm respectively.

Material	Duration	Thickness (μm)
PMMA	4 hr 5 hr 7 hr	4.43 4.93 5.26
PS	30 mins 60 mins 120 mins	4.35 4.58 5.07

Table.1 Thickness of coated films by CBD

Material	rpm	Duration (mins)	Thickness (μm)
PMMA	2500 3000	140 120	3.17 3.1
PS	2000 3000	120 80	7.75 5.45

Table.2 Thickness of coated films by Spin coating

Sample	Position (2θ) deg	β (deg)	d- spacing	r (Å)
PMMA	31.6625	0.0502	2.82596	3.5295
	76.5972	0.8029	1.24393	1.5536
Composite	31.6647	0.2007	2.82578	3.5292
	36.4440	0.4015	2.46542	3.0792

Table.3 XRD parameters of Sample II and Sample III

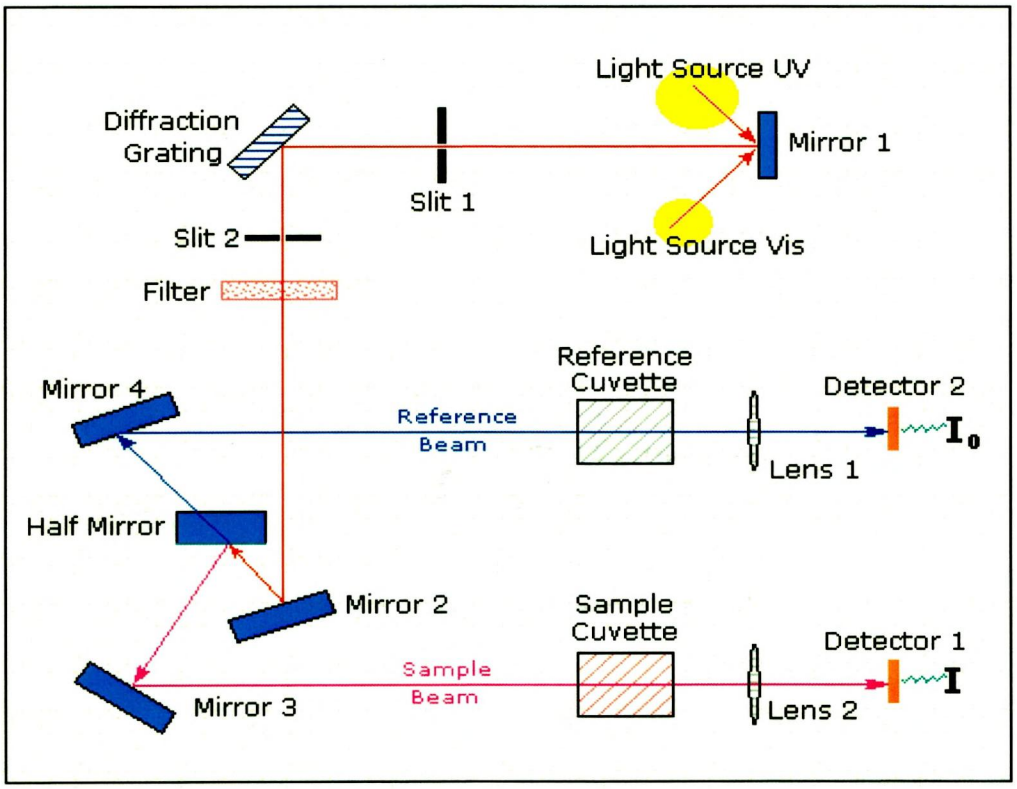

Figure 4.1 Schematic diagram of UV-Visible Spectrophotometer

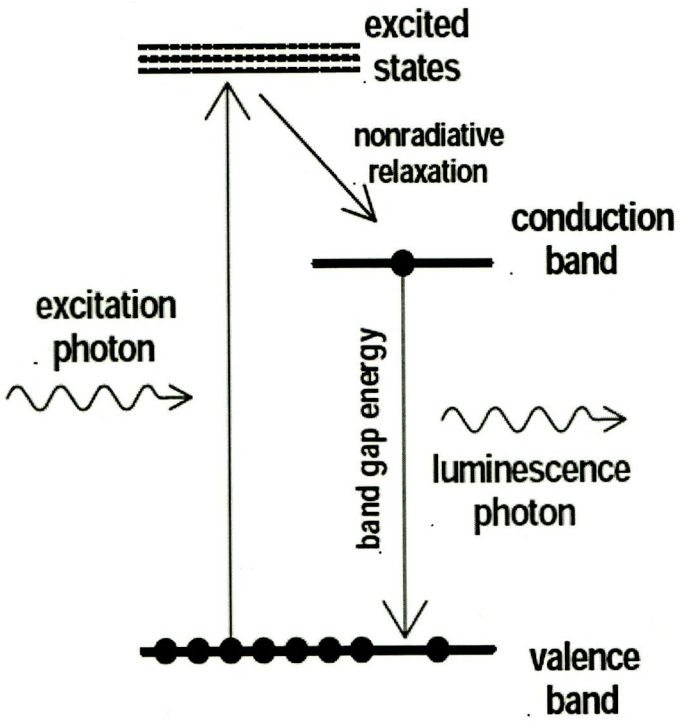

Figure.4.2 Basic principle of photoluminescence process

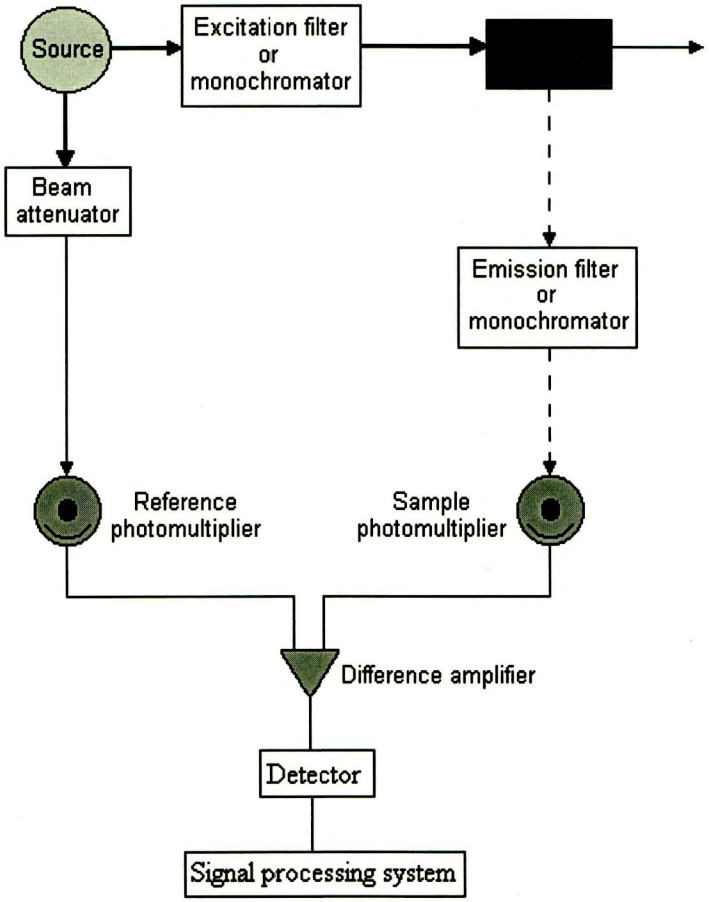

Figure.4.3 Photoluminescence spectrometer.

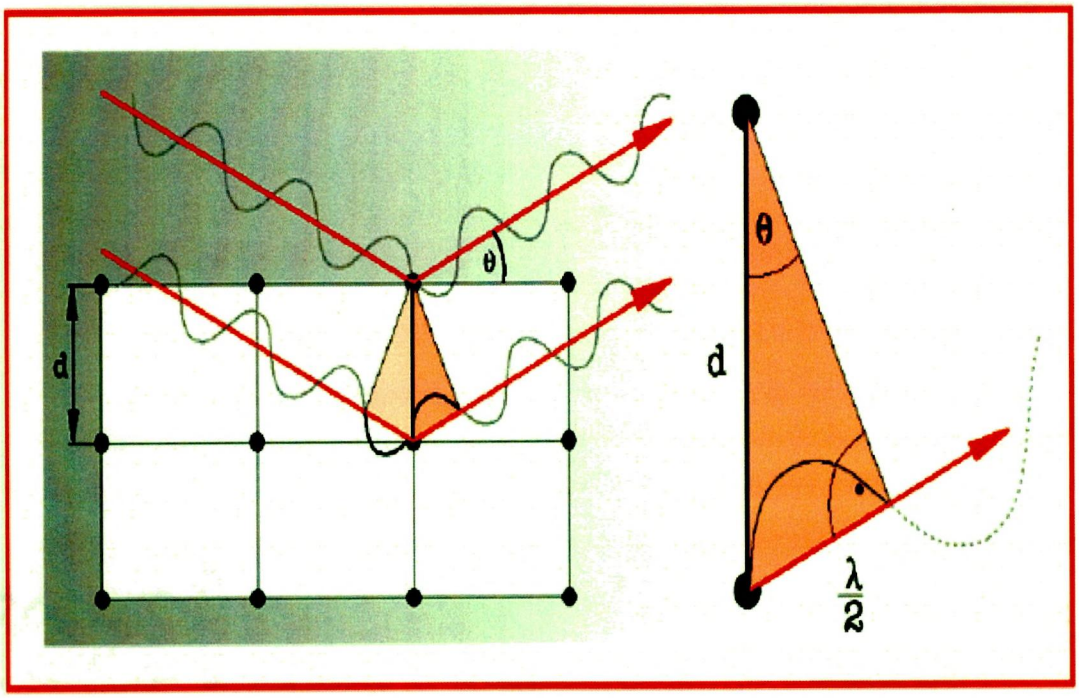

Figure.4.4 Bragg's X-ray diffraction.

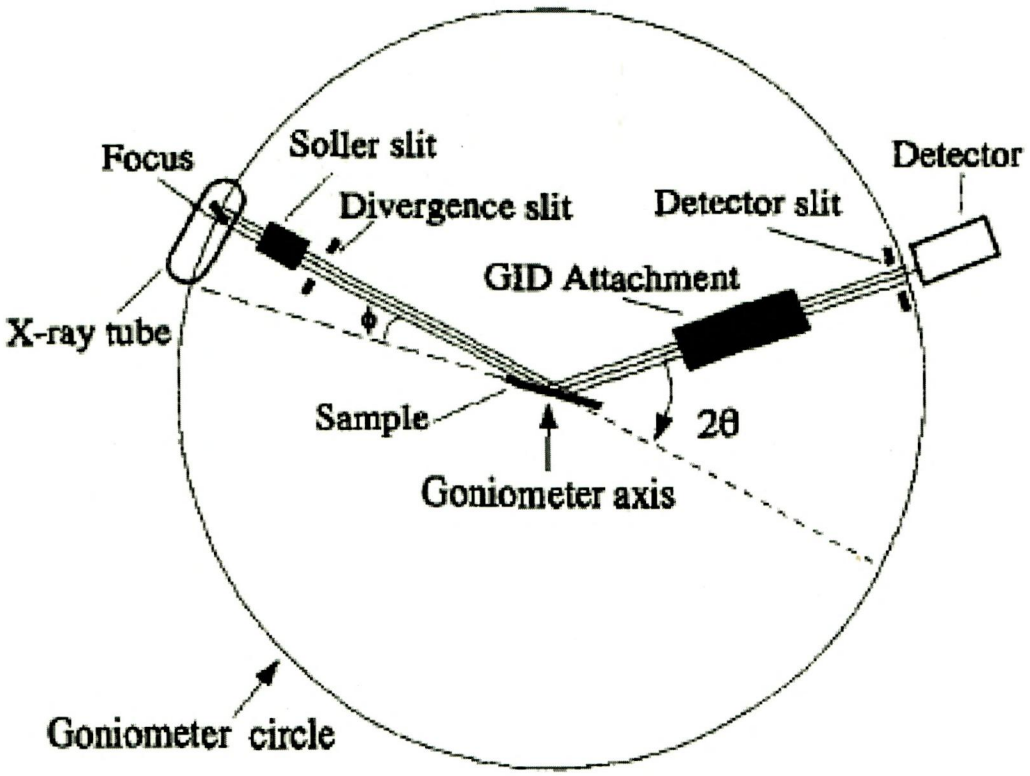

Figure.4.5 X-ray difractrometer

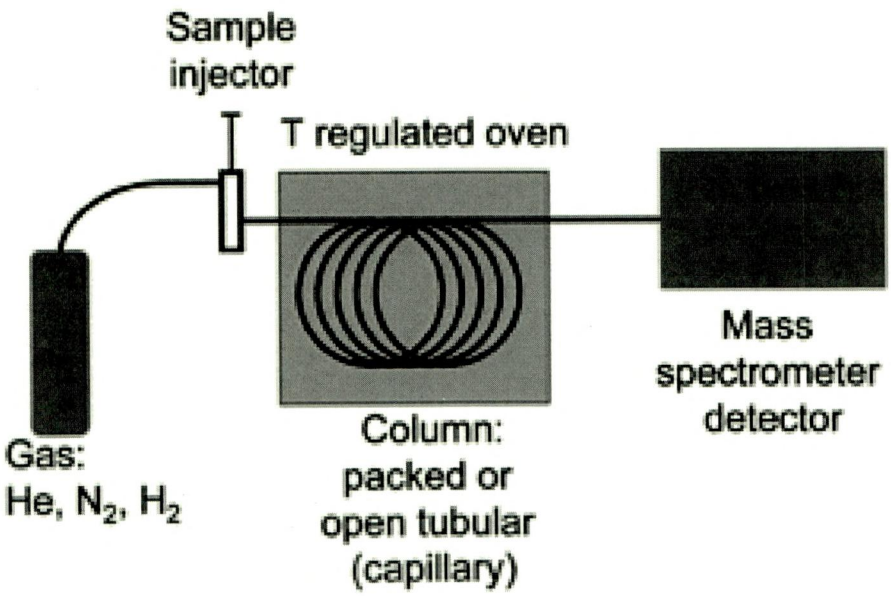

Figure.4.6 Schematic representation of GC-MS spectrometer

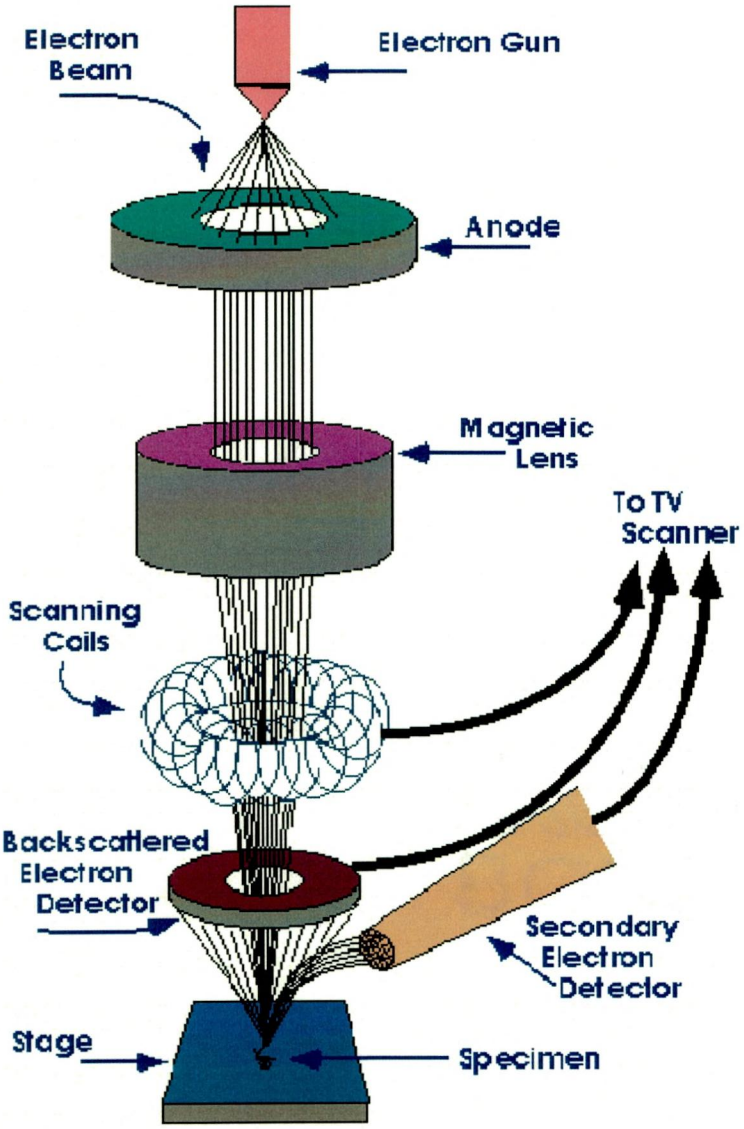

Figure.4.7 Schematic representation of Scanning Electron Microscope

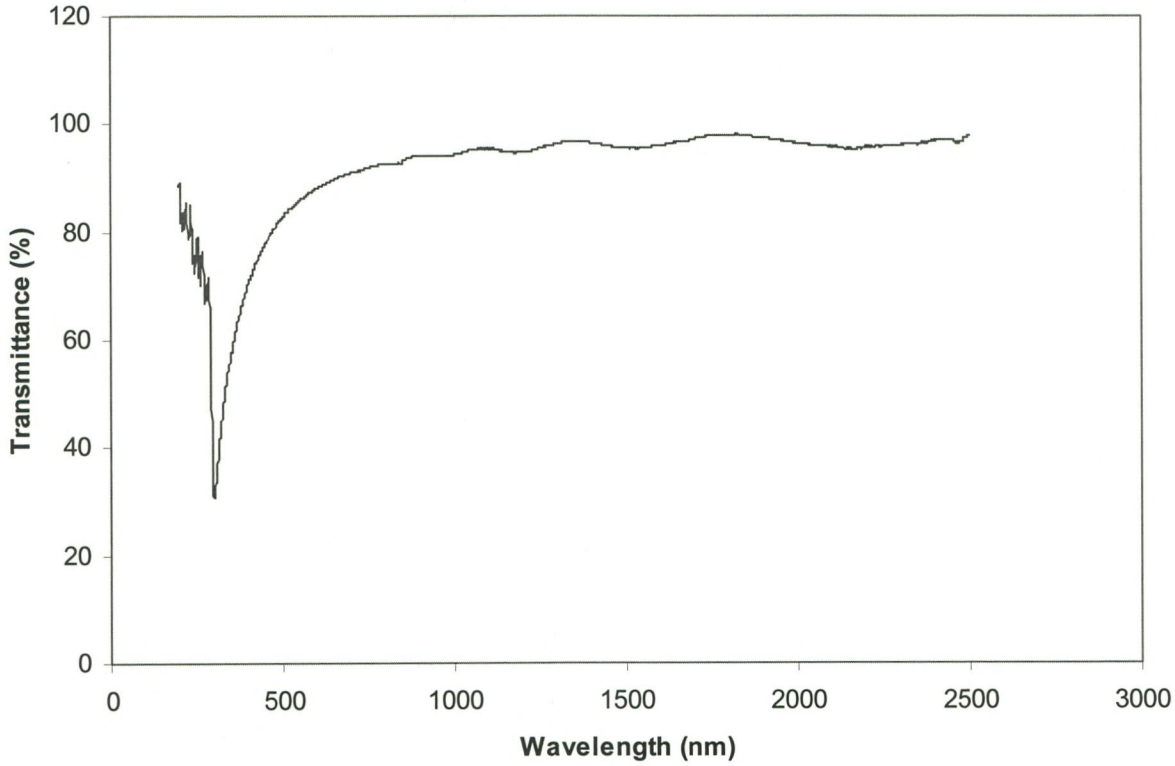

Figure 4.8 Transmittance spectrum of PS film

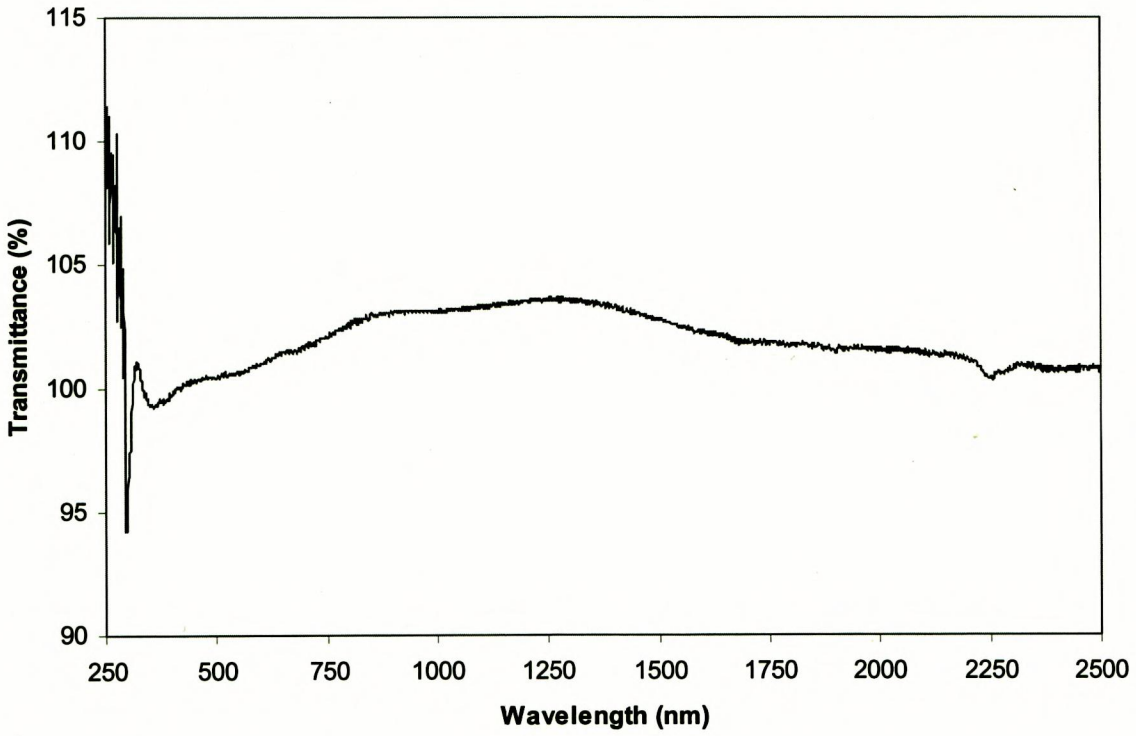

Figure 4.9 Transmittance spectrum of PMMA film

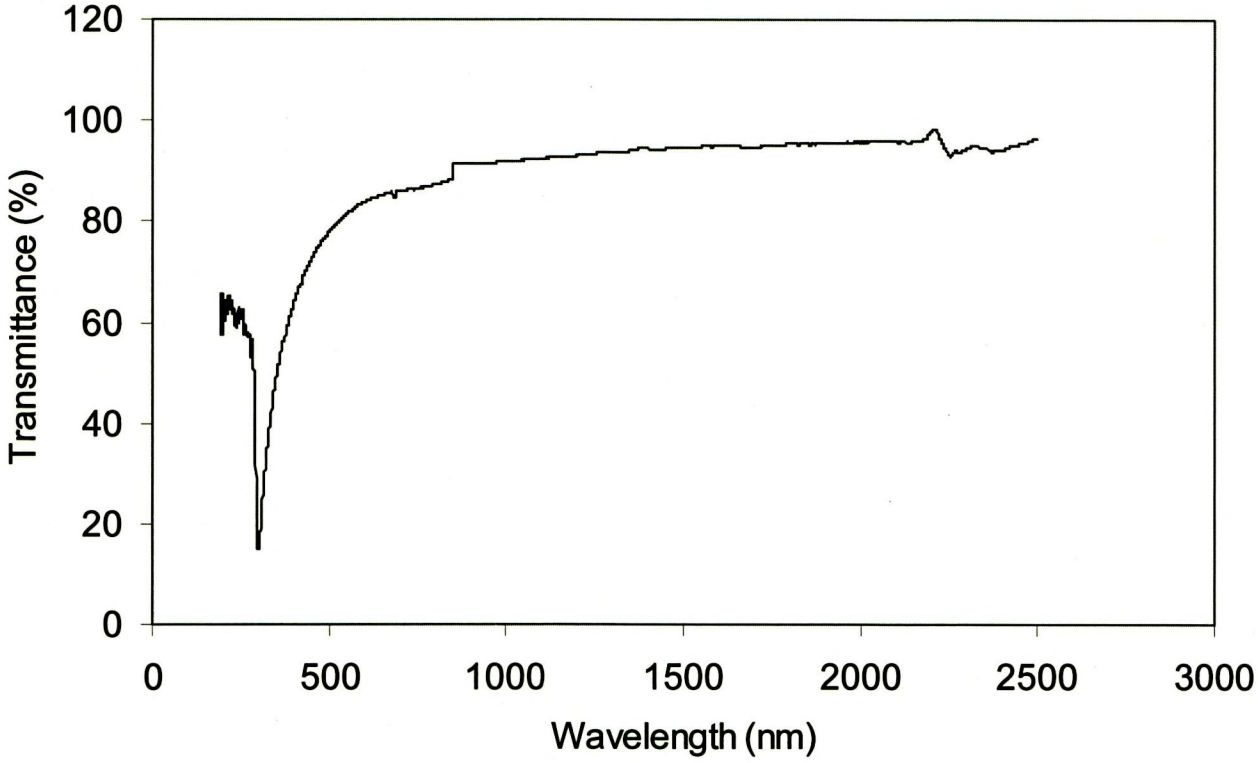

Figure 4.10 Transmittance spectrum of composite film

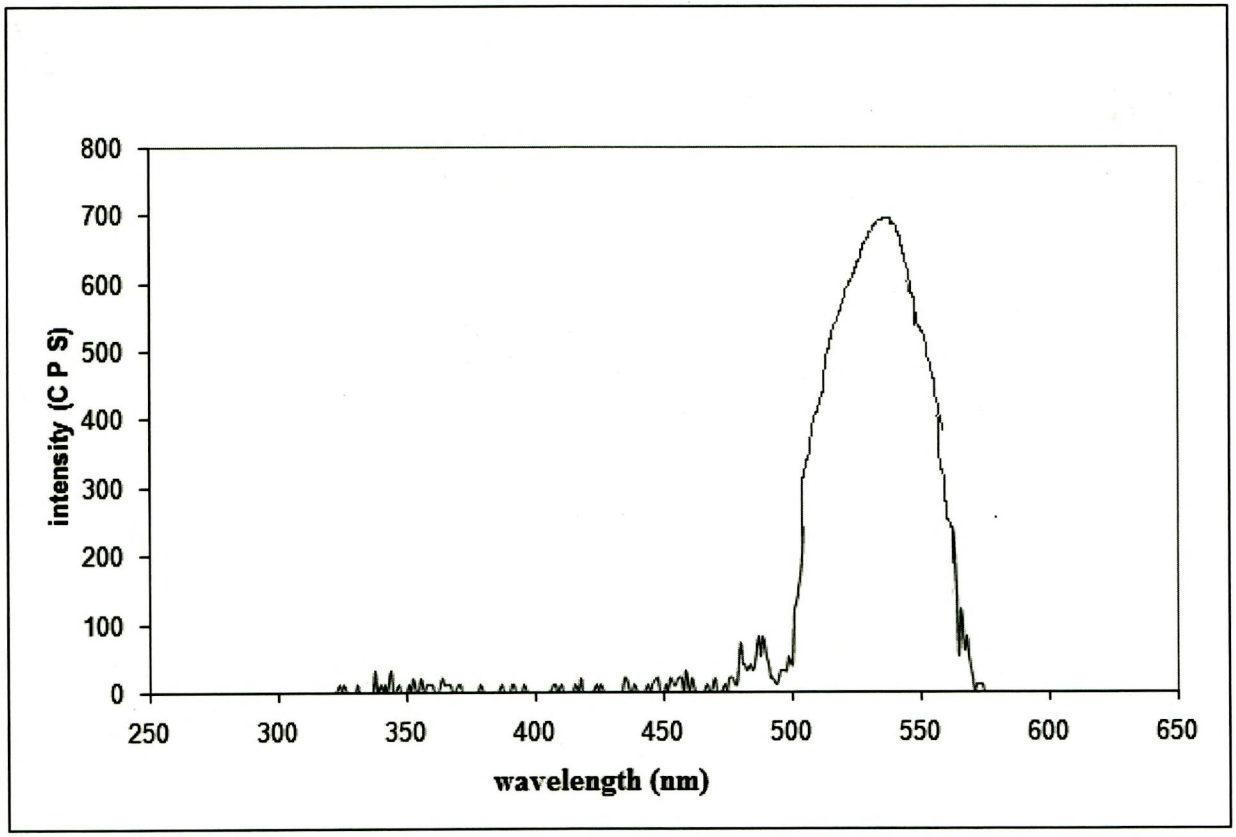

Figure 4.11 Photoluminescence spectrum of PS film

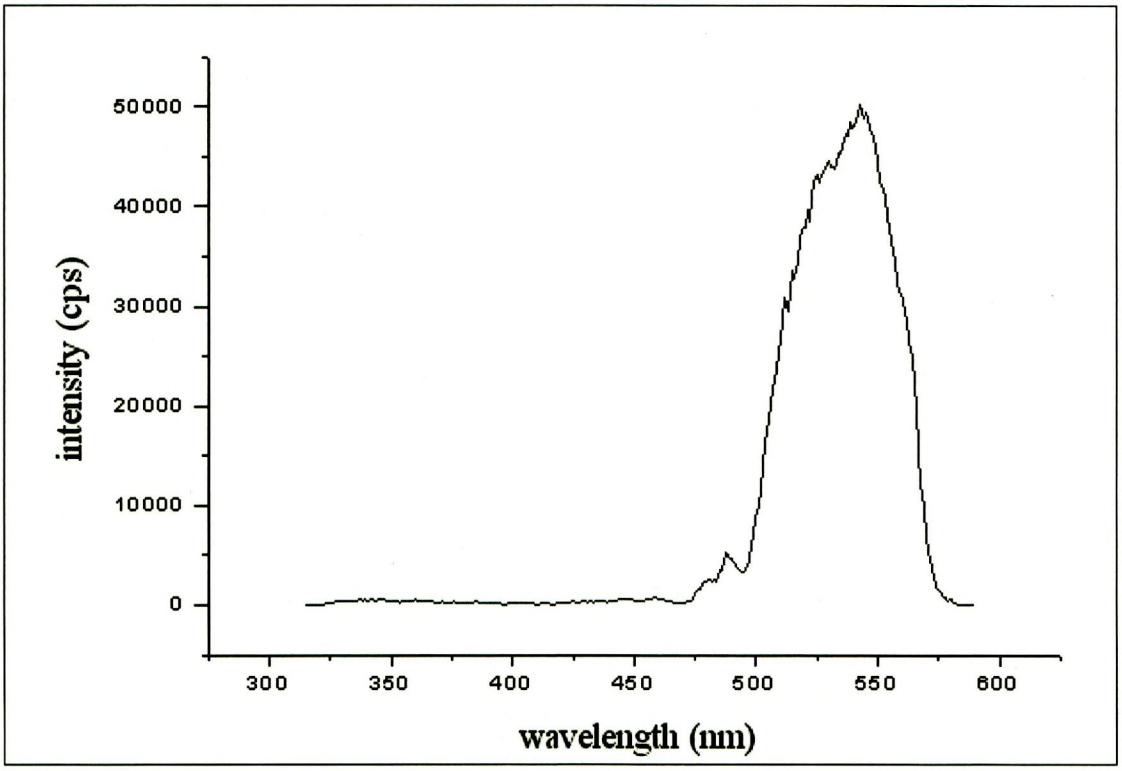

Figure 4.12 Photoluminescence spectrum of PMMA film

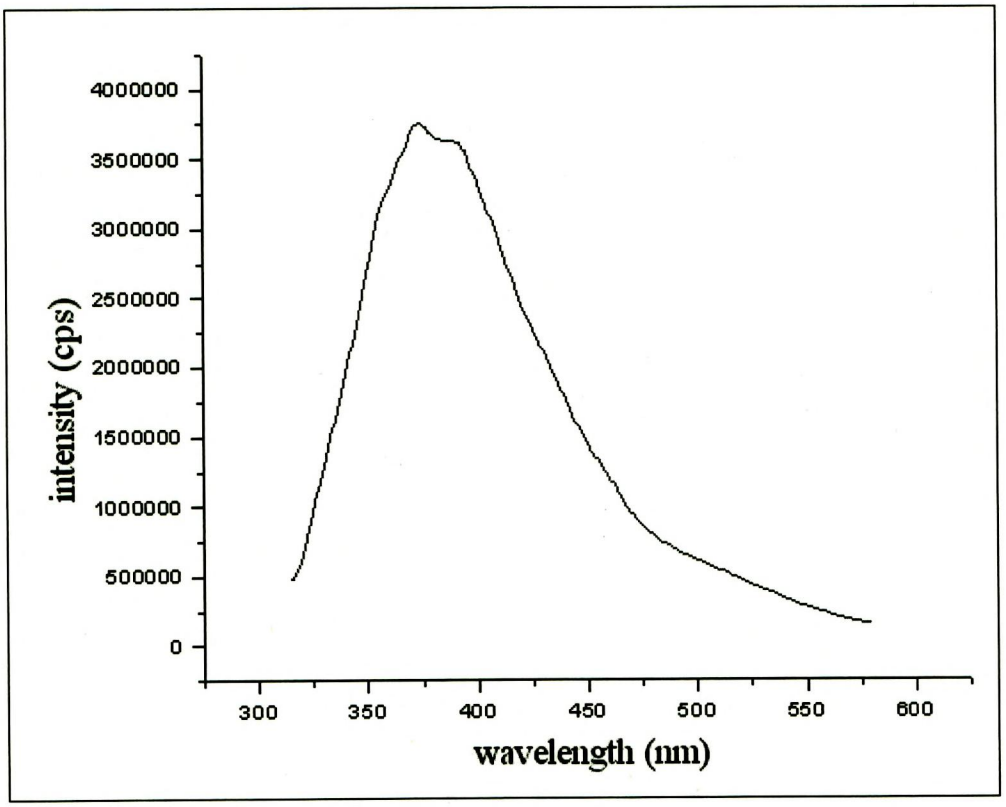

Figure 4.13 Photoluminescence spectrum of composite film

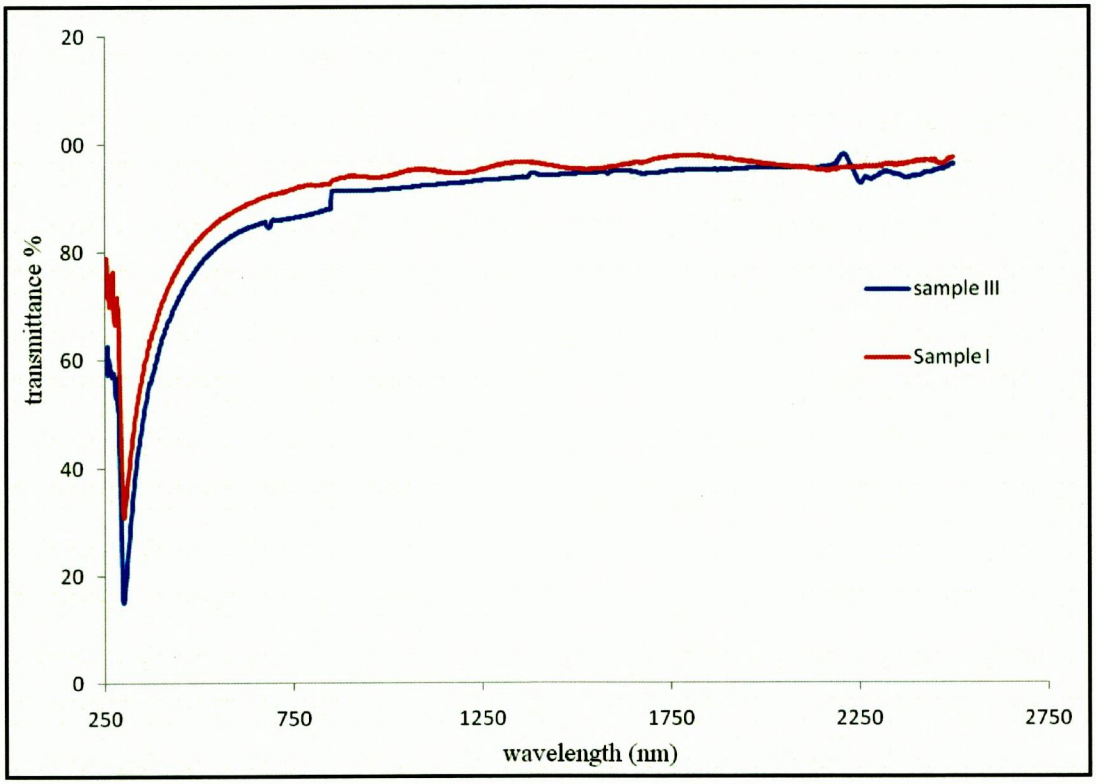

Figure 4.14 Representation of shift in bandgap

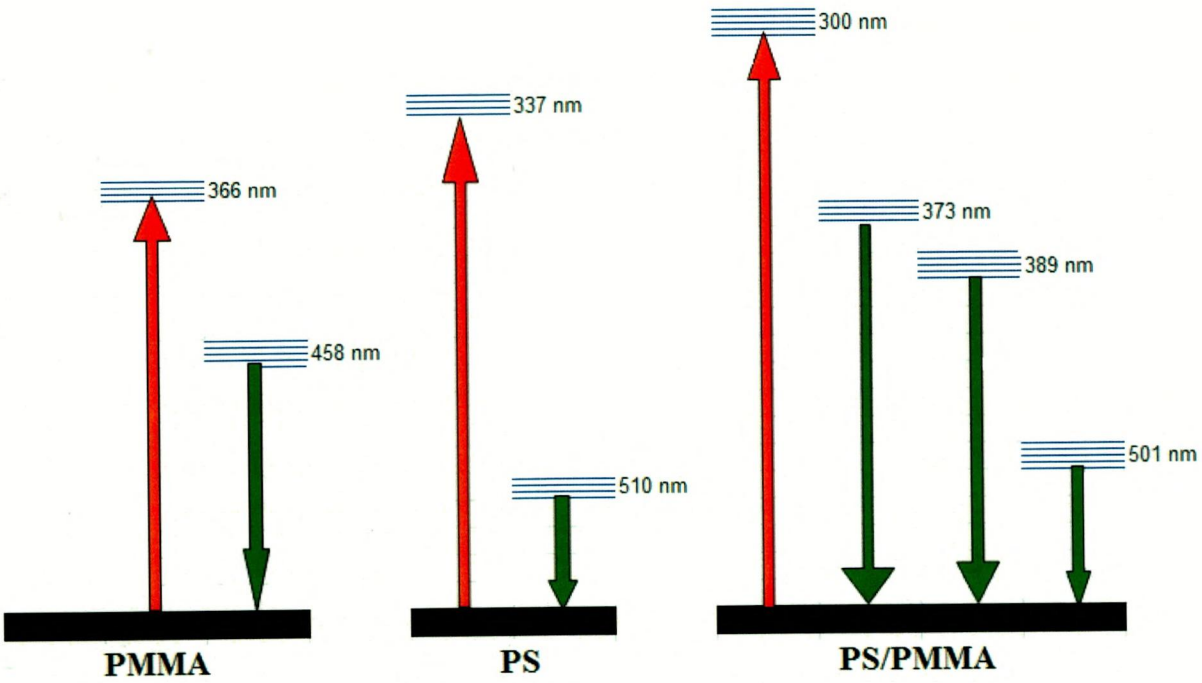

Figure.4.15 Energy level diagram

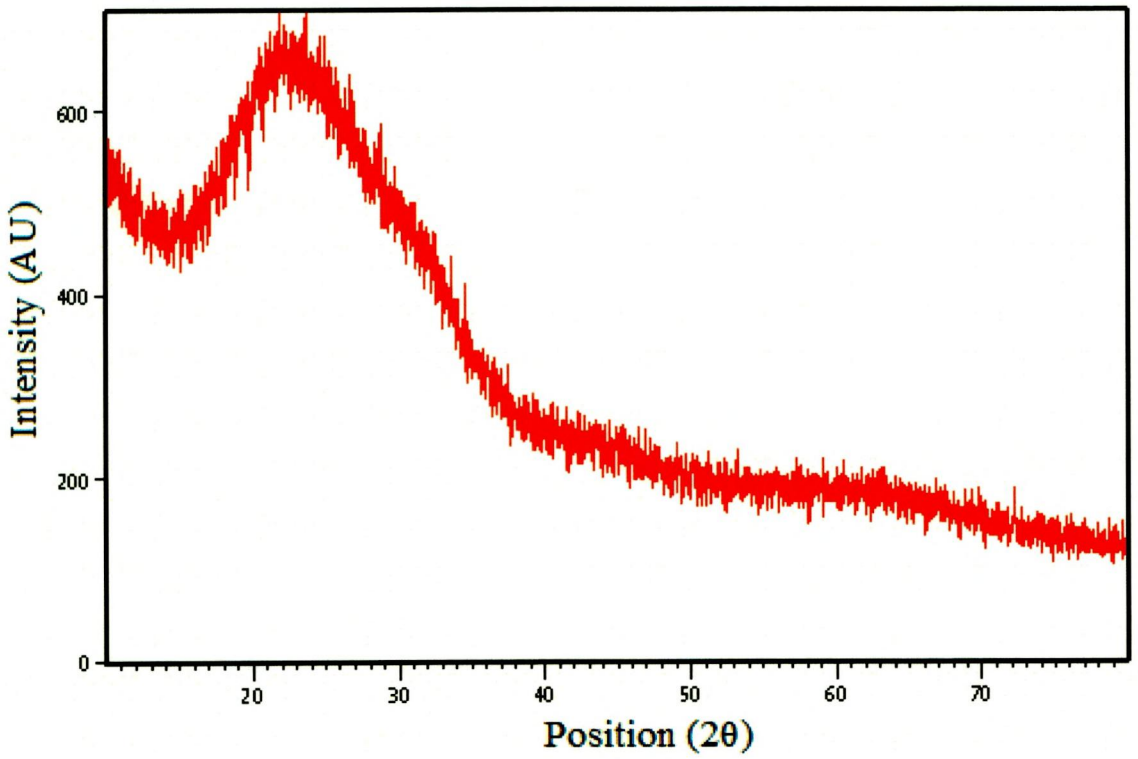

Figure.4.16 XRD pattern of Sample I

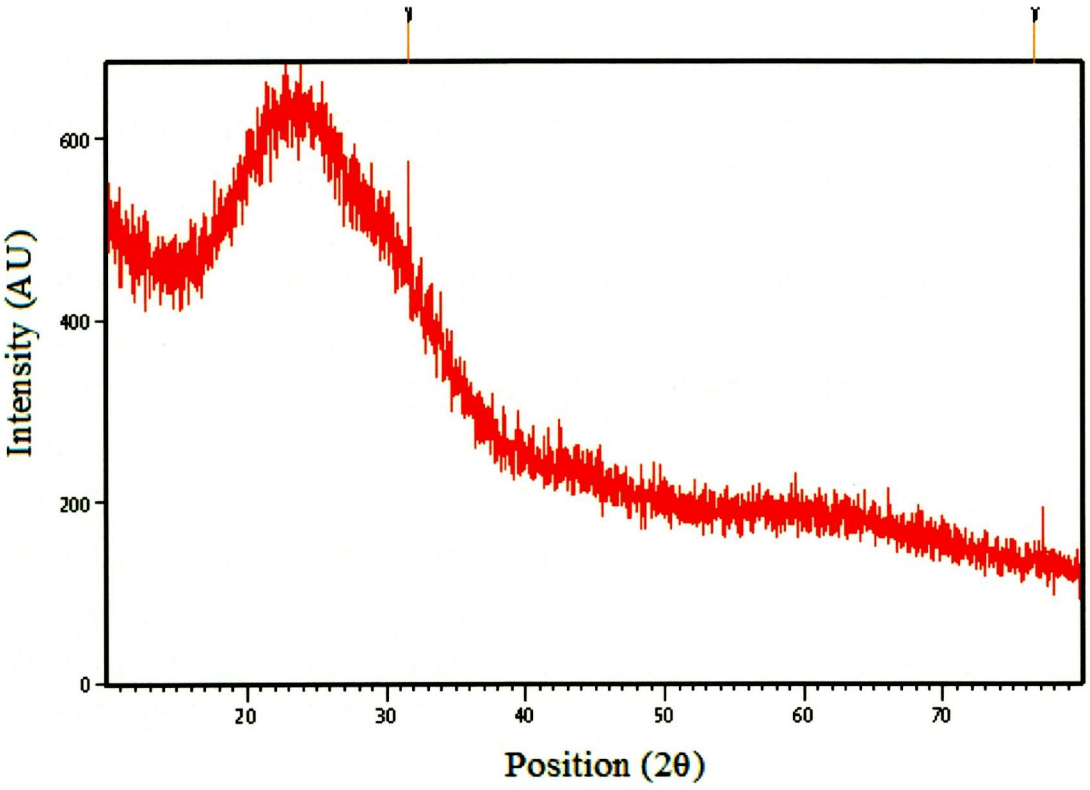

Figure.4.17 XRD pattern of sample II

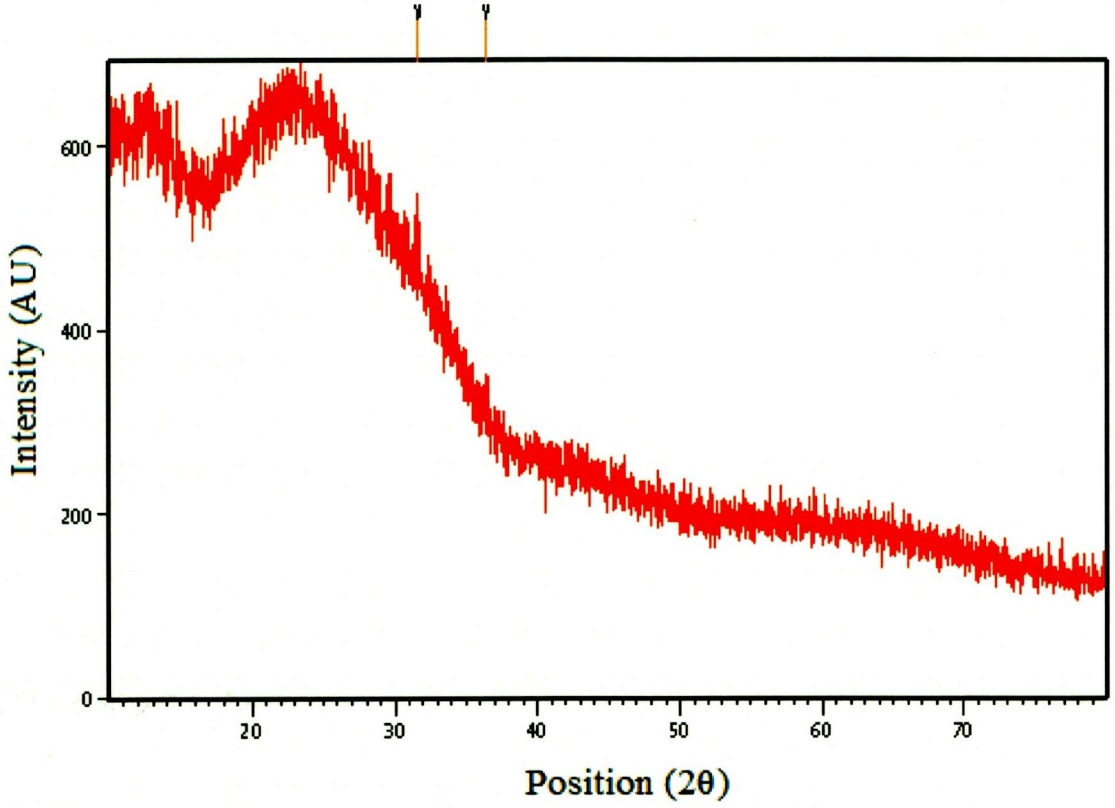

Figure.4.18 XRD pattern of Sample III

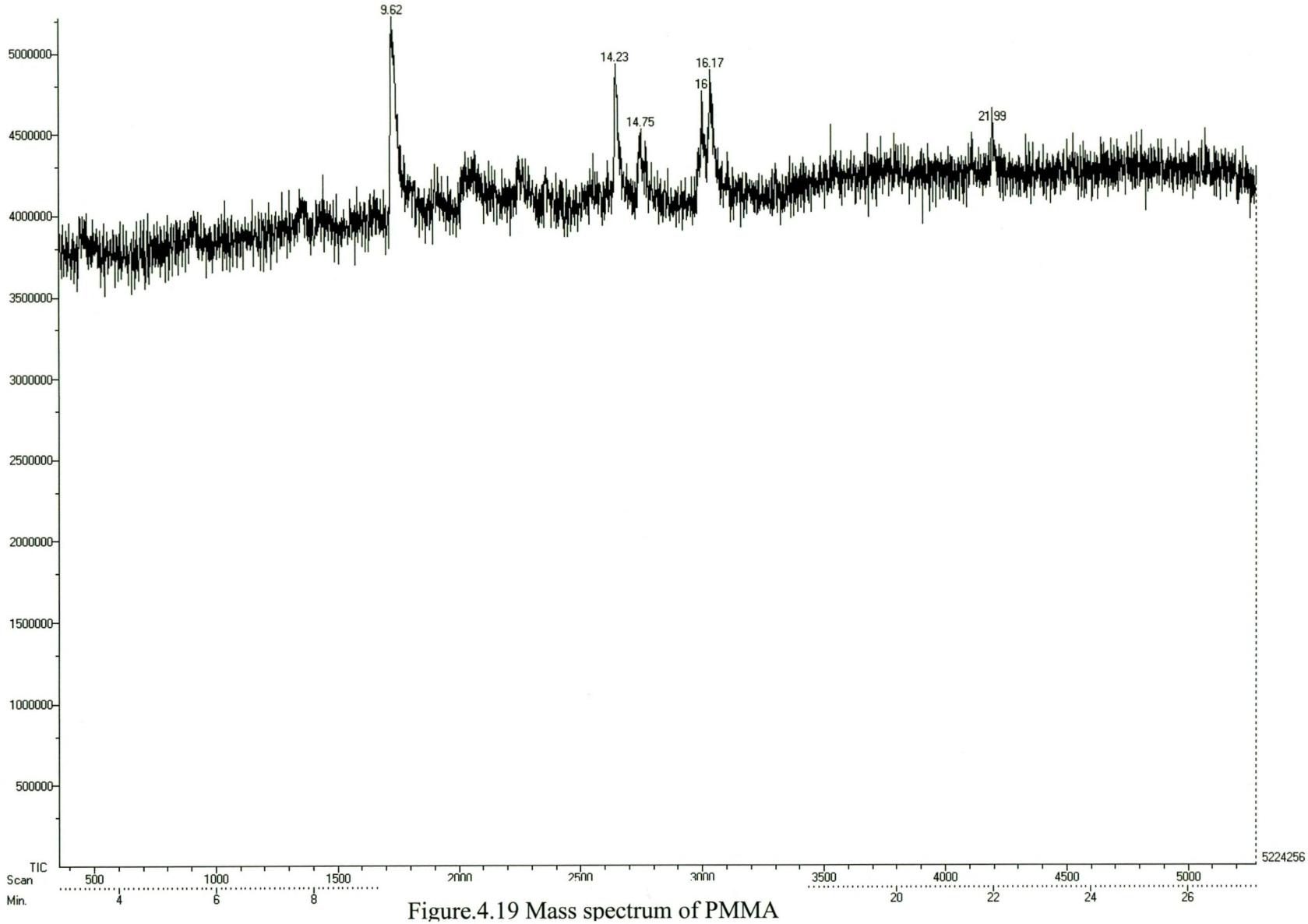

Figure.4.19 Mass spectrum of PMMA

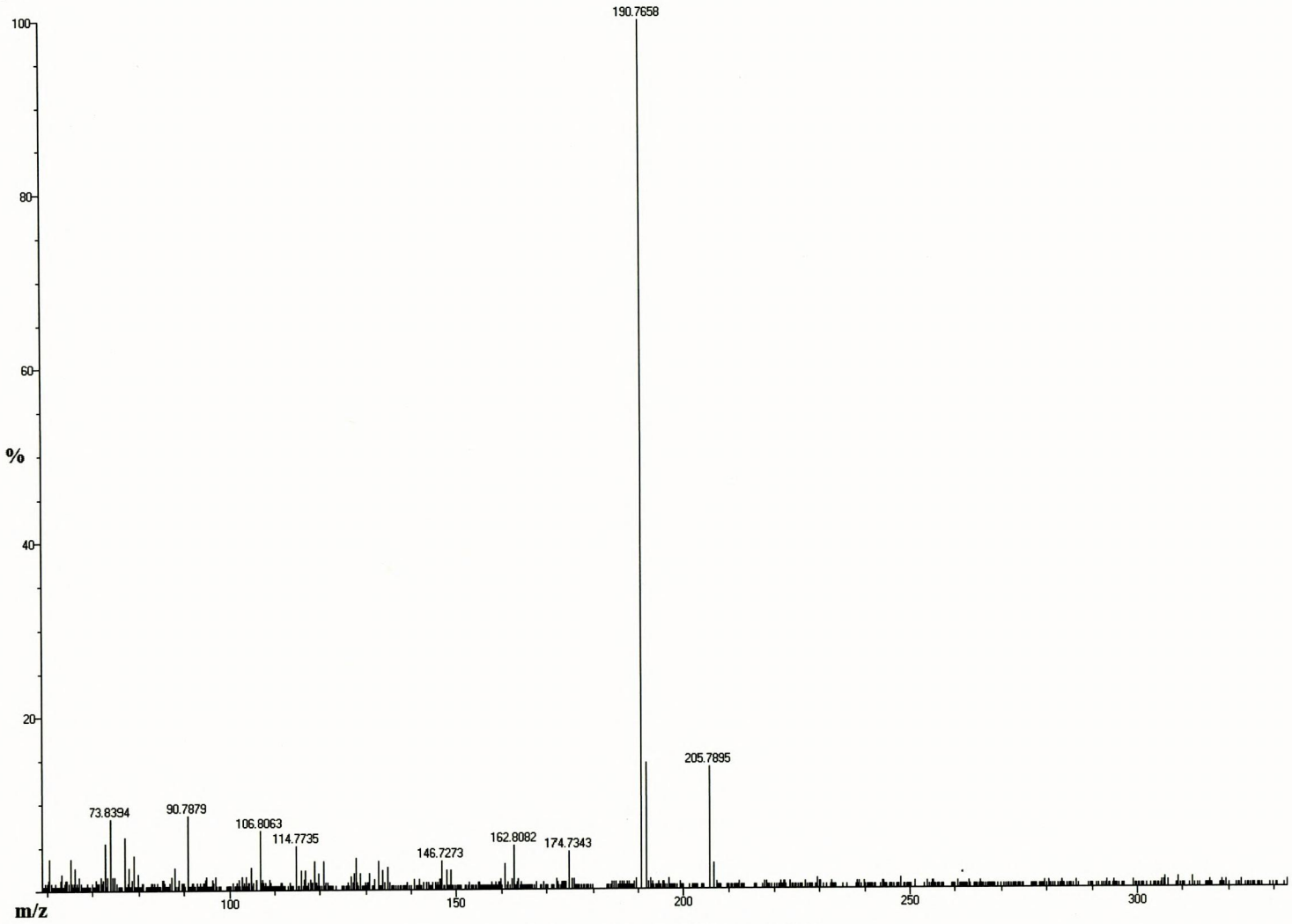

Figure.4.20 Mass spectrum of GC peak at 9.62

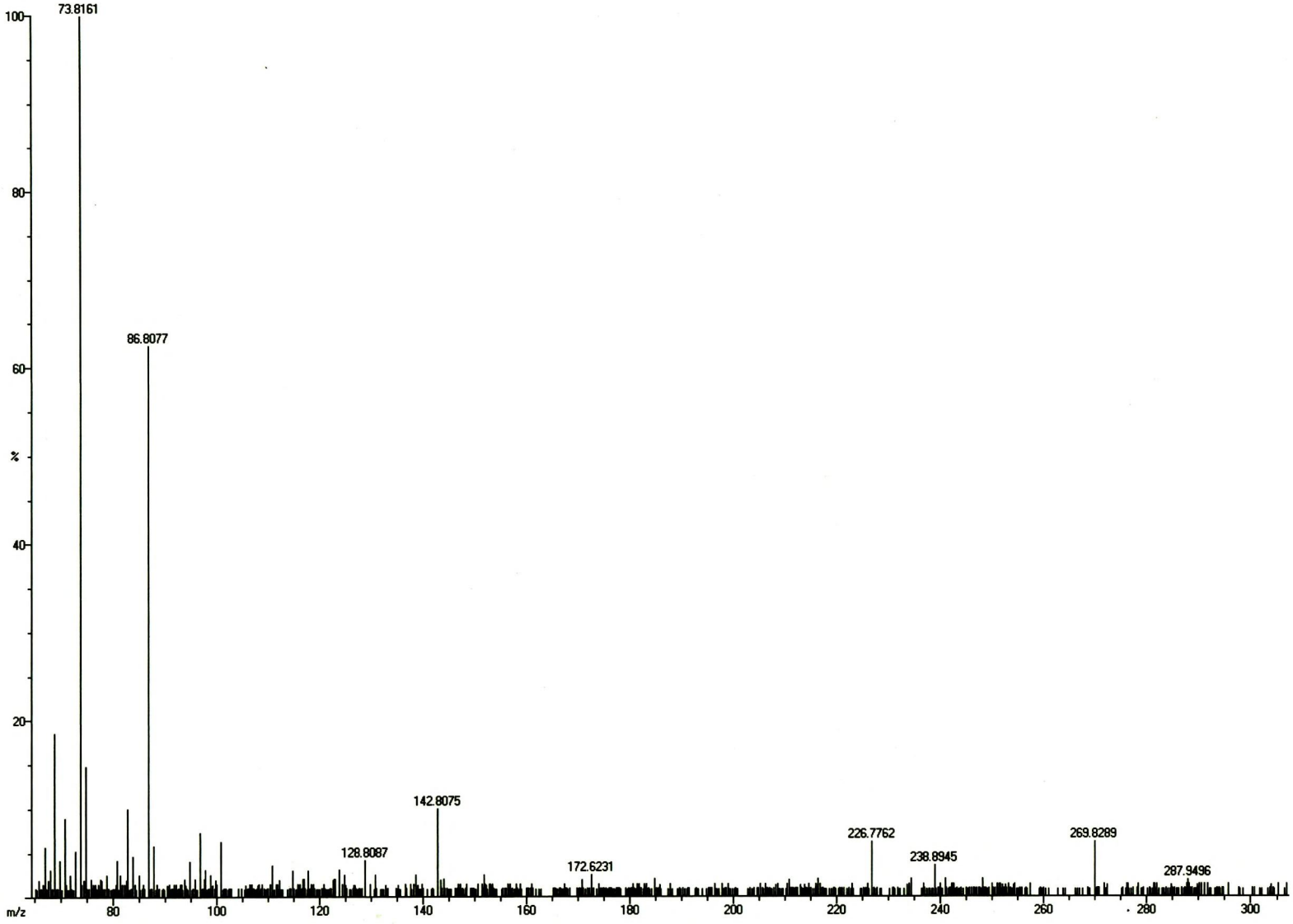

Figure.4.21. Mass spectrum of GC peak at 14.23

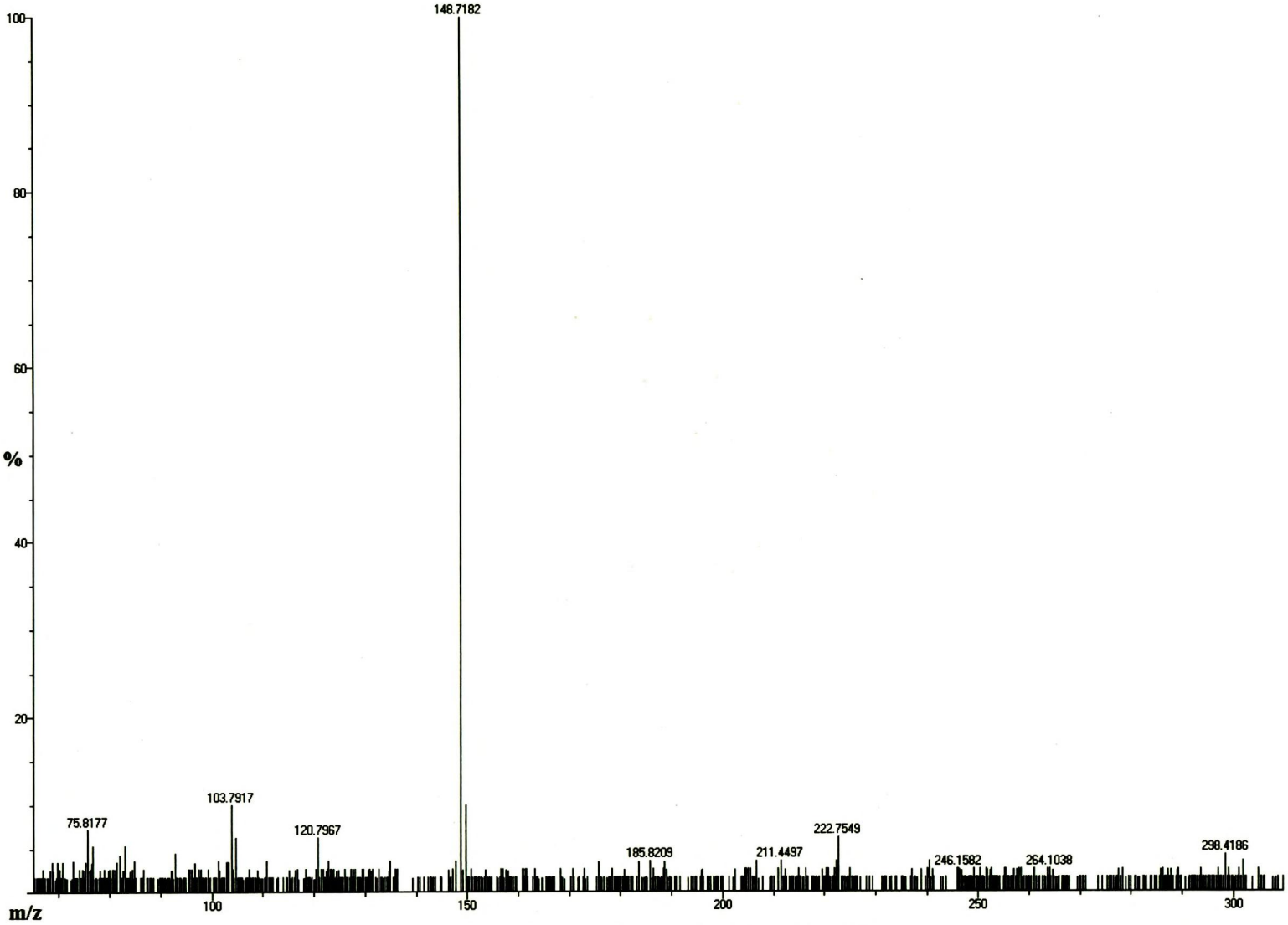

Figure.4.22 Mass spectrum of GC peak at 14.75

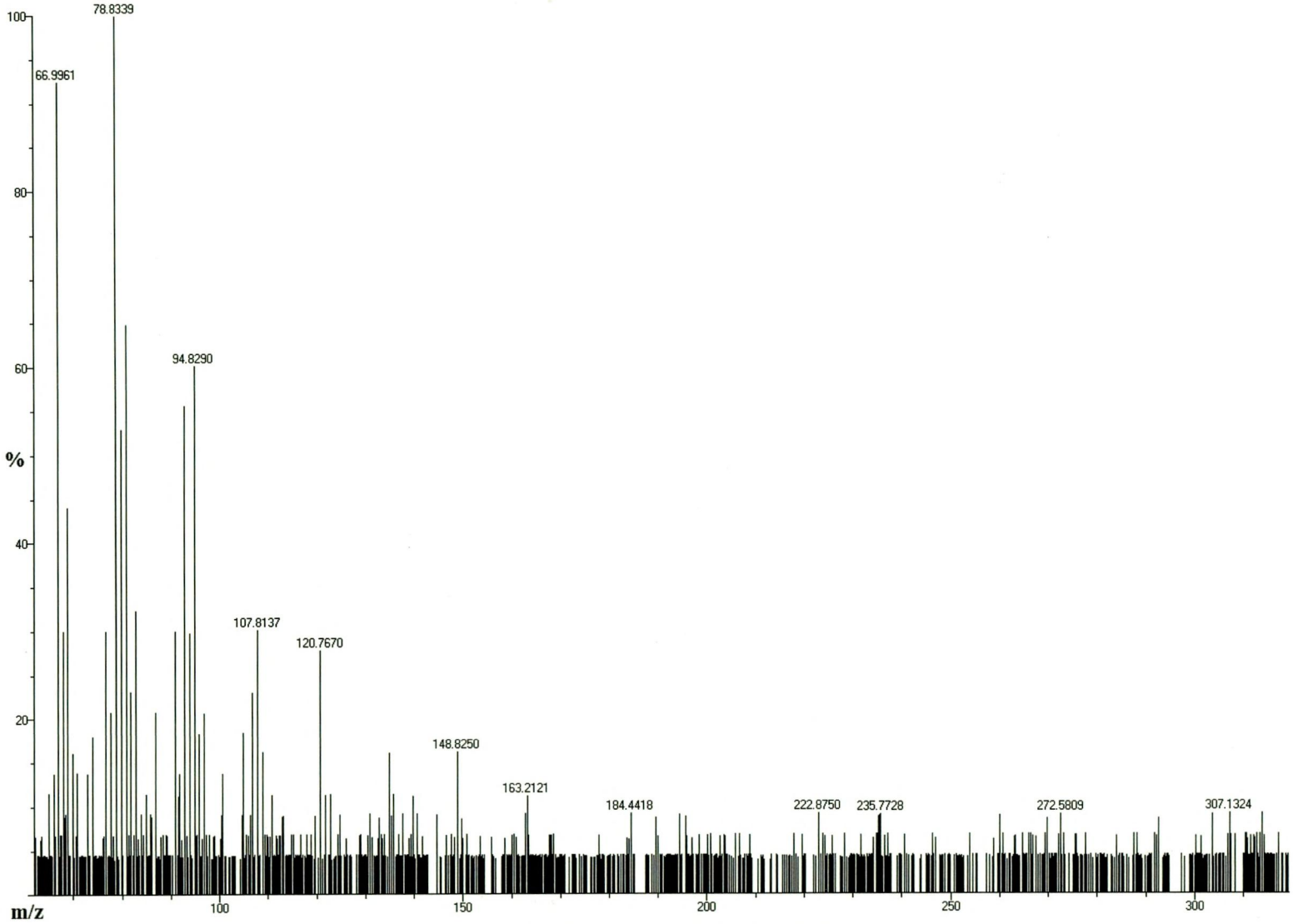

Figure.4.23. Mass spectrum of GC peak at 16

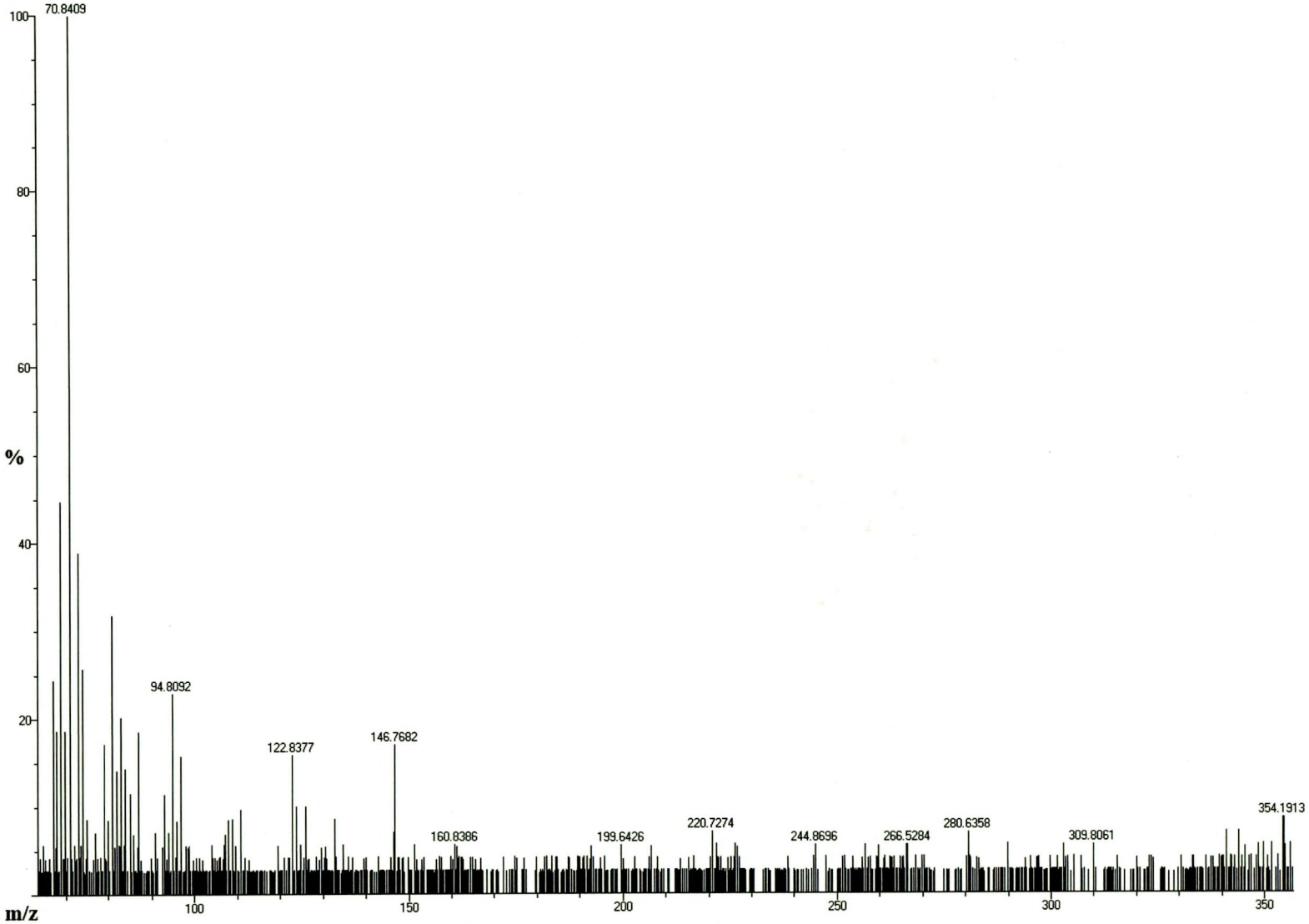

Figure.4.24. Mass spectrum of GC peak at 16.17

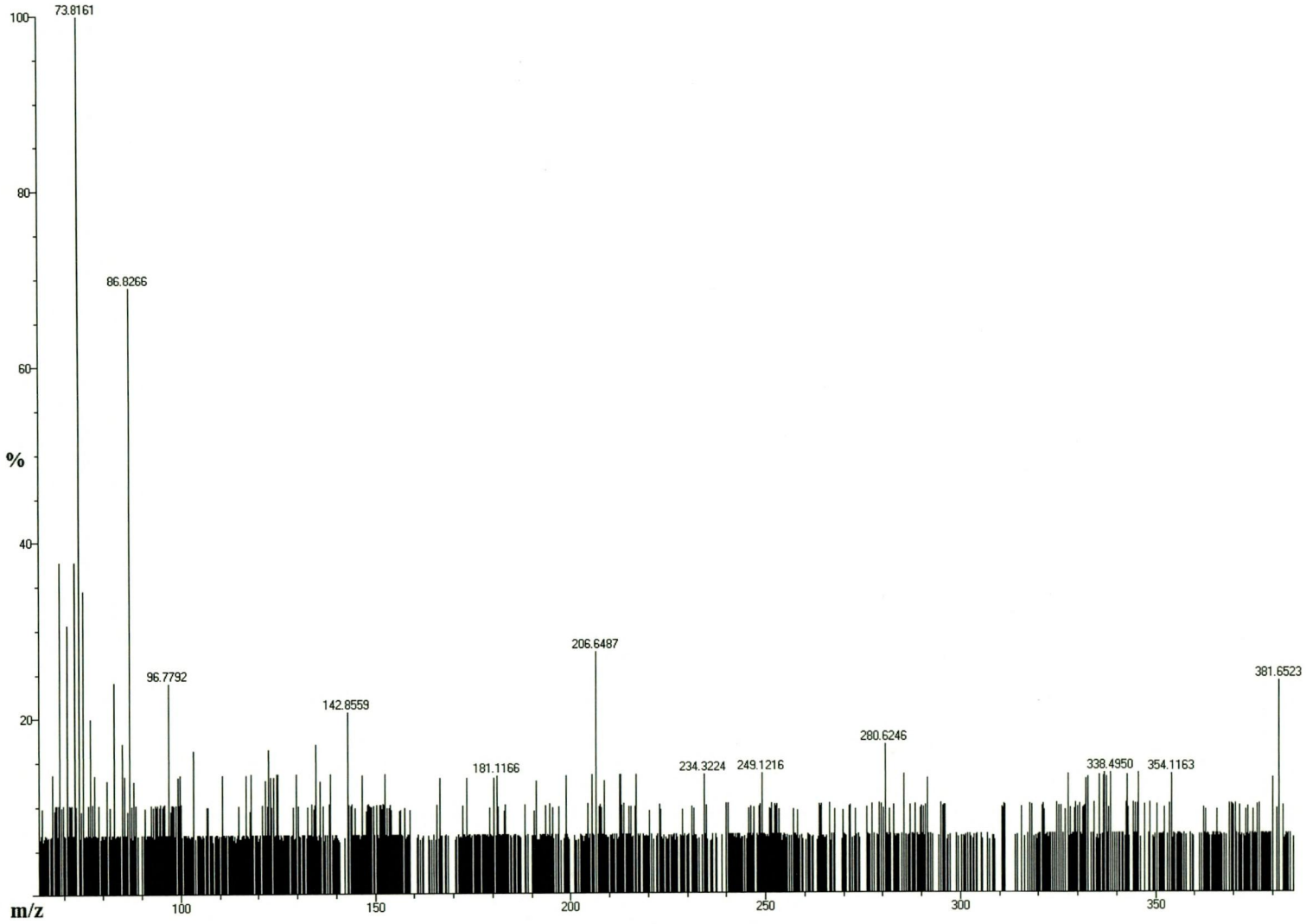

Figure.4.25. Mass spectrum of GC peak at 21.9 9

Figure 4.26 SEM Image of PS/PMMA composite film

References

- **Patania V.B**, Spectroscopy, Campus Book International, 2004.
- **P.S.Kalsi**: Spectroscopy of organic compounds: 2009; pg 9-10.
- **Skoog, et al.** Principles of Instrumental Analysis. 6th ed. Thomson Brooks/Cole. 2007, Pg 351.
- **Y.Anjaneyulu, K.Chandrasekhar, Valli manikam**; A textbook of Analytical chemistry, 2006; pg 673.
- **Milton ohring,** Materials science of thin films Deposition and Structure; 2006, pg 6-7 &594-595.
- **Leon I. Maissel and Reinhard Glang**, Hand book of Thin film technology, 1983, Pg-19-24.
- **Supriya S. Mahajan**, Instrumental Methods of Analysis, G.H prints Pvt. Ltd, first edition, 2010, Pg 155.
- **Frank A. Settle,** Handbook of Instrumental Techniques for Analytical Chemistry, Prentice Hall PTR (ECS Professional), 1997, Pg 609-613.
- **M.G. Arora, M. Singh, M.S. Yadav**; Polymer Chemistry, Anmol publications Pvt. Ltd, 2003, Pg 171-172.
- **K.L.N. Deepak, R.Kuladeep, S. Venugopal Rao, D. Narayana Rao**; Luminescent microstructures in bulk and thin films of PMMA, PDMS, PVA, and PS fabricated using femtosecond direct writing technique, Chemical Physics Letters, Vol 503, Year 2011, Pg 57-60.